Published in final edited form as:

Nanotechnology. 2010 February 10; 21(6): 065102. doi:10.1088/0957-4484/21/6/065102.

Rose Bengal-decorated silica nanoparticles as photosensitizers for inactivation of gram-positive bacteria

Yanyan Guo[1], **Snezna Rogelj**[2], and **Peng Zhang**[1,3]

[1]Department of Chemistry, New Mexico Tech, Socorro, NM 87801, USA

[2]Department of Biology, New Mexico Tech, Socorro, NM 87801, USA

Abstract

A new type of photosensitizer, made from Rose Bengal (RB)-decorated silica (SiO_2–NH_2–RB) nanoparticles, was developed to inactivate gram-positive bacteria, including Methicillin-resistant *Staphylococcus aureus* (MRSA), with high efficiency through photodynamic action. The nanoparticles were characterized microscopically and spectroscopically to confirm their structures. The characterization of singlet oxygen generated by RB, both free and immobilized on a nanoparticle surface, was performed in the presence of anthracene-9,10-dipropionic acid. The capability of SiO_2–NH_2–RB nanoparticles to inactivate bacteria was tested *in vitro* on both gram-positive and gram-negative bacteria. The results showed that RB-decorated silica nanoparticles can inactivate MRSA and *Staphylococcus epidermidis* (both gram-positive) very effectively (up to eight-orders-of-magnitude reduction). Photosensitizers of such design should have good potential as antibacterial agents through a photodynamic mechanism.

1. Introduction

Staphylococci are spherically shaped gram-positive bacteria that are usually arranged in grape-like microscopic clusters. Although more than 20 species of *Staphylococcus* exist, *Staphylococcus aureus* and *Staphylococcus epidermidis* are two of the most significant species as they are involved in a large number of human-related diseases. Although *S. epidermidis* is usually non-pathogenic, it can cause infections in patients with a compromised immune system or a long-term indwelling catheter. *S. aureus* is pathogenic, causing a wide variety of infections especially in burn wound patients. In particular, Methicillin-resistant strains of *S. aureus* (MRSA), which are resistant to all but one or two antibiotics, are one of the major causes of hospital-acquired infections causing significant infections and morbidity world-wide. An increasing concern about the growing resistance of MRSA to conventional antimicrobial agents is leading to tremendous efforts aimed towards the development of alternative approaches for the treatment and prevention of MRSA infections.

Photodynamic therapy (PDT) has been identified as one of the viable approaches for bacterial photoinactivation [1–3]. First introduced in the 1990s to treat cancers [4–6], PDT

[3]Author to whom any correspondence should be addressed: pzhang@nmt.edu.

involves the delivery of lethal drugs to the targets (tumors or microbes) by the combination of a light-activatable chemical (photosensitizer), light, and oxygen [7–9]. Upon exposure to illumination of appropriate wavelengths, the photosensitizer is excited from a lower-energy 'ground state' to a higher-energy 'triplet state', which can then react with molecular oxygen in the surroundings, generating reactive oxygen species (ROS) [10]. Such ROS, and singlet oxygen in particular, can cause damage to the plasma membranes and DNA, eventually leading to cell death [11, 12]. Examples of photodynamic inactivation of various gram-positive and gram-negative bacteria, such as *S. aureus* [13–16], *Streptococcal* species [17, 18], *Escherichia coli* [17], *Porphyromonas gingivalis* [19], and *Pseudomonas aeruginosa* [20], have been documented in the literature. The advantage of using PDT for treating and controlling MRSA infections over conventional antimicrobials lies in the fact that MRSA is unlikely to develop resistance to photochemically induced killing, which, among other ROS, is mediated predominantly by singlet oxygen [21].

The synthesis and development of photosensitizer, the key element in effective PDT, has drawn tremendous academic and industrial interest in recent years. For antimicrobial applications, a good photosensitizer should ideally possess such features as: (1) high quantum yield of generating singlet oxygen or other ROS; (2) minimal or no dark toxicity, and (3) good specificity or selectivity towards the target(s).

The object of the present study was to develop nanoparticle-based photosensitizers that would display high efficacy in inactivating a group of bacteria under *in vitro* conditions. We found silica nanoparticles decorated with Rose Bengal (RB), a well-known photosensitizing molecule [22, 23], to be highly efficient in inactivating gram-positive bacteria, MRSA. and *S. epidermidis*, through photodynamic action. The results show promise for these nanoparticles to be tested under *in vivo* conditions.

2. Experimental details

2.1. Chemicals and materials

Rose Bengal (4,5,6,7-tetrachloro-2′,4′,5′,7′-tetraiodofluoresce in disodium salt) (RB), tetraethyl orthosilicate (TEOS), and 3-aminopropyltriethoxysilane (APTS) were purchased from Sigma-Aldrich. 2-(4-morpholino)-ethane sulfonic acid (MES), 1-ethyl-3-(3-dimethylaminopropyl) carbodiimide HCl (EDC), Triton X-100, ammonium hydroxide (29.6 wt%), cyclohexane, n-hexanol, isopropyl alcohol, LB Broth, and LB Agar were purchased from Fisher Scientific. Disodium salt of 9,10-anthracenedipropionic acid (ADPA) was purchased from Invitrogen. Phosphate buffered saline (PBS) was purchased from GIBCO. All chemicals were used as-received without further purification. The bacteria used in this study were MRSA (gram-positive, ATCC No. BAA-44), and *S. epidermidis.* (gram-positive, ATCC No. 35984). Transmission electron microscopy (TEM) grids were from Electron Microscopy Sciences, PA.

2.2. Synthesis and characterization of Rose Bengal-decorated silica nanoparticles

The Rose Bengal-decorated silica nanoparticles (denoted as SiO_2–NH_2–RB hereafter) were prepared in three steps. First, pure SiO_2 nanoparticles were synthesized by hydrolysis of

TEOS in reverse microemulsion. Second, the silica surface was functionalized with amine groups. Lastly, RB dye molecules were covalently conjugated to the silica surface. To begin with, 1.77 g of Triton (X-100) was mixed with 1.6 ml of n-hexanol, 7.5 ml of cyclohexane, and 480 μl of deionized water under vigorous stirring. After the solution became transparent, 60 μl of ammonium hydroxide (29.6 wt%) was added to the solution. The solution was subsequently sealed and stirred for 20 min, followed by adding 100 μl of TEOS and stirring for 24 h. A large amount of ethanol (~20 ml) was then added to break the microemulsion. Silica nanoparticles were then recovered by centrifuging at 14 000 rpm for 10 min, and washed with acetone three more times and twice with dionized (DI) water. The nanoparticles were finally dispersed in DI water.

The silica surface was functionalized with amine groups by the following procedures. 10 mg of silica nanoparticles were dispersed into 20 ml of isopropyl alcohol, and the mixture was sonicated for 30 min. Next, 1 ml of NH_4OH (29.6 wt%) was added into the mixture under stirring for 20 min. 5 μl of APTS was subsequently added under stirring. Amine-functionalized silica (SiO_2–NH_2) nanoparticles were collected via centrifugation after 3 h. Alternatively, the silica surface could be functionalized with amine groups directly in one-pot during the synthesis of the nanoparticles. In that case, before breaking the microemulsion during the synthesis with ethanol, 5 μl of APTS was added to the microemulsion while stirring and was further incubated overnight. The SiO_2–NH_2 nanoparticles were then recovered by adding ethanol to break the microemulsion and centrifuging, followed by rigorous washing with acetone and DI water.

The conjugation of RB to the SiO_2–NH_2 nanoparticles was carried out as follows. 10 μl of RB solution (1.6 mM) was added to 3 ml of MES buffer (0.1 M, pH 6.0), followed by adding 5–8 mg of EDC into the mixture. The RB–EDC conjugation reaction was allowed to proceed at room temperature for 20 min. Separately, 1 ml (~12 mg ml^{-1}) of SiO_2–NH_2 nanoparticles were washed twice with 1 ml of the above MES buffer. After the second wash, the pellet was re-dispersed in 2 ml of MES buffer. Subsequently, the SiO_2–NH_2 nanoparticle dispersion and RB solution were combined under stirring for 3 h at room temperature. The mixture was then centrifuged and pellet washed with DI water. After the third wash, the pellet of SiO_2–NH_2–RB nanoparticles was re-dispersed in 1 ml DI water and was ready for use.

2.3. TEM characterization of SiO_2–NH_2–RB nanoparticles

A drop of nanoparticle suspension was deposited on a Formvar-covered carbon-coated copper grid, and allowed to dry at room temperature. TEM images were taken on a JEOL 2010 high resolution transmission electron microscope.

2.4. IR characterization of SiO_2–NH_2–RB nanoparticles

A drop of nanoparticle suspension in ethanol was deposited on a plate of NaCl, and allowed to dry at room temperature. Infrared absorption spectra were taken on a Nicolet Nexus 8700 Fourier transform infrared (FTIR) spectrometer.

2.5. Measurement of singlet oxygen ($^1O_2$)

The detection of singlet oxygen, generated by free RB dye in solution, was similar to had been described previously [24]. In brief, 10 μl of 1.6 mM RB solution and 3 ml of 5 μM ADPA solution were mixed in a cuvette under stirring, and placed onto a Photon Technology International (PTI) spectrofluorometer. The fluorescence intensity of ADPA at 400 nm, when excited at 374 nm, was recorded. The solution was then irradiated at 525 nm for 2 min, and another reading at 400 nm (excited at 374 nm) was taken. The irradiation/measurement cycle was repeated for 20–30 min. The intensity of the 525 nm light from the xenon lamp associated with the spectrofluorometer and used to irradiate the solution was 60 μW, as measured by a power meter (SPER Scientific Laser Power Meter 840011). The measurement of singlet oxygen generated by the SiO_2–NH_2–RB nanoparticles was carried out in a similar manner, with the concentration of RB on the nanoparticles kept the same as that in the case of free RB solution.

2.6. Bacterial culture

Bacteria were grown in sterile LB broth in an orbital shaker at 37 °C. Following a 20 h incubation period, the bacteria were grown to ~10^8 CFU ml^{-1} and confirmed by a colony count. Bacteria were washed twice with PBS solution before they were used in photosensitization tests.

2.7. In vitro photosensitization tests

10 μl of bacterial suspension (~10^8 CFU ml^{-1}) and 20 μl of SiO_2–NH_2–RB (~10^{13} NPs ml^{-1}, 6 mg ml^{-1}) were added to 70 μl of LB broth, and then the suspension incubated at 37 °C for 30 min with shaking. The following control groups were treated in a similar manner: bacteria only, bacteria treated with pure SiO_2 nanoparticles, bacteria treated with NH_2-functionalized SiO_2 nanoparticles (SiO_2–NH_2) and bacteria treated with free RB solution. All tests were performed in duplicate.

A light source (Lumacare, LC122A, MBG Technologies Inc., Newport Beach, CA) with a 525 nm bandpass filter, which has a measured ~14 mW cm^{-2} output (equivalent to 1×10^{-4} einstein m^{-2} s^{-1}), was used for illumination. During the lamp illumination period, all samples were placed on ice so as to slow down the growth of bacteria and avoid any overheating. The surviving fraction of the bacteria was characterized by a colony count. The colony count was performed by serial dilution and a spread plate. Each sample was done in duplicate and each experiment was repeated three times. The average CFU value was calculated.

3. Results and discussion

3.1. Design of nanoparticles

Silica-based nanoparticles function as good carriers for the delivery of photosensitizers due to their following attractive features. First, silica nanoparticles are water dispersible. Second, they are chemically and photodynamically stable. Third, the silica surface can be easily modified with different functional groups. Various types of target-recognition molecules can then be effectively decorated onto the silica nanoparticle surface following well-known and

facile conjugation chemistry. Moreover, silica nanoparticles are transparent and usually do not alter the spectral characteristics of the photosensitizers. Finally, and equally importantly, silica nanoparticles help decrease the self-quenching of the photosensitizers, possibly by immobilizing and appropriately spacing the dye molecules. This results in higher photostability of the immobilized photosensitizers as compared to free photosensitizers in solution. Therefore, in this study, we chose silica nanoparticles as the carriers for the photosensitizers.

Silica nanoparticles are generally synthesized by Stöber's sol–gel method [25, 26], where the alkoxysilane compounds, such as TEOS and tetramethyl orthosilicate (TMOS), hydrolyze under basic or acidic conditions. The subsequent condensation reaction forms a stable alcosol in an ammonia/HCl–ethanol–water mixture. However, in this study, silica nanoparticles were synthesized by the controlled hydrolysis of TEOS in reverse microemulsion systems, which allows for the subsequent NP surface functionalization with amine groups to be carried out in a one-pot reaction.

Microemulsions are transparent solutions formed by spontaneously mixing oil and water with appropriate surfactants, sometimes with the assistance of a cosurfactant [27, 28]. These systems comprise a large number of oil-in-water (o/w) or water-in-oil (w/o) droplets of uniform nanometer sizes. By controlling the reactions that take place within such droplets, one can synthesize monodisperse nanoparticles using microemulsions. Since the hydrolysis of TEOS takes place in the aqueous phase, reverse (w/o) microemulsions were adopted in this study.

The photosensitizing molecule used in this study is 4,5,6,7-tetrachloro-2′,4′,5′,7′-tetraiodofluorescein (Rose Bengal, RB), a widely used anionic photosensitizing molecule with a good quantum yield of singlet oxygen generation[4]. The covalent attachment of RB to the silica nanoparticle surface was realized through the conjugation between the carboxylic groups (COO^-) of the RB dye molecules and the amine groups ($–NH_2$) pre-functionalized on the nanoparticle surface. The schematic diagram of the resulting $SiO_2–NH_2–RB$ nanoparticle is shown in figure 1.

3.2. Characterization

A TEM image of the $SiO_2–NH_2–RB$ nanoparticles is shown in figure 2(a). The results showed that the diameters of most of the particles were in the range of 50–80 nm. The covalent binding between RB and the $SiO_2–NH_2$ nanoparticle surface was confirmed by IR measurement as shown in figure 2(b). The sharp band around 1190 cm^{-1} in the $SiO_2–NH_2–RB$ nanoparticles could be assigned to the C–N bond between RB and the surface amine group. The excitation and emission spectra of RB are shown in figure 3. There were two excitation peaks at wavelengths around 508 and 546 nm. Their emission was observed at around 562 nm. $SiO_2–NH_2–RB$ displayed similar excitation and emission bands as free RB dye in solution. Through back titration using ultraviolet–visible (UV–vis) absorption, we estimated that ~50% of RB added to the conjugation mix had actually attached to the silica nanoparticles.

4Fluorescein, 3,4,5,6-tetrachloro-2′,4′,5′,7′-tetraiodo-, dianion (Rose Bengal dianion, RB). Available from [29].

The characterization of RB, free or decorated on SiO_2 nanoparticles, as a source of singlet oxygen ($^1O_2$) under illumination, was performed through the photobleaching of ADPA in aqueous solution. When the ~375 nm-absorbing ADPA molecule reacts with $^1O_2$ to form endoperoxide, its fluorescence at 400 and 420 nm decreases. By monitoring the disappearance of the ADPA fluorescence, one could indirectly detect the generation of $^1O_2$ from the photosensitizers. Note that there was no interference between the wavelength used to excite ADPA (374 nm) and that used to illuminate the photosensitizer (525 nm).

It has been shown in previous reports that the intensity decrease of ADPA emission follows an exponential decay over time, as ADPA is being quenched by the generated singlet oxygen. The data points in figure 4 could be fitted into exponential decay functions, suggesting that the kinetics of the singlet oxygen generation of both free RB and RB-decorated nanoparticles is very similar to that of other silica-based nanoparticles described in the literature [24, 30, 31]. It can be seen from figure 4 that the fluorescent intensity of ADPA initially decreased faster for free RB than for SiO_2–NH_2–RB. This indicates that free RB has a higher quantum yield of generating singlet oxygen than SiO_2–NH_2–RB in the first few minutes of irradiation. The quantum yield of generating singlet oxygen of free RB was reported to be approximately 0.75 in H_2O and air (see footnote 4). The quantum yield of generating singlet oxygen of SiO_2–NH_2–RB was thus determined to be approximately 0.6, using $\Phi_\Delta = \Phi_\Delta\,(\mathrm{St}) \times S(U)/S(\mathrm{St})$ [32], where St represents the standard, U the unknown, Φ the quantum yield, and S the slope of the linear fit for the initial data points. This value for SiO_2–NH_2–RB NPs is higher than 0.43 that was reported earlier for RB bound to micron-size polymer beads [33]. The higher quantum yield of generating singlet oxygen using SiO_2–NH_2–RB nanoparticles, as compared to the polymer-based RB microparticles, is probably due to the smaller SiO_2–NH_2–RB particle size, leading to more surface area and easier access of RB to the molecular oxygen present in the solution.

3.3. Bactericidal action of SiO_2–NH_2–RB

The use of free RB solution in photodynamic inactivation of a number of bacterial species had long been reported in the literature [23, 34]. It was found that some gram-positive bacteria (*Bacillus subtilis*, *S. aureus*, *Streptococcus faecalis* and *Streptococcus salivarius*) were inactivated by free RB dye ~200 times more quickly than the gram-negative *Salmonella typhimurium*. RB immobilized on polystyrene beads also displayed photodynamic inactivation of *E. coli* [35] with a typical ~99.99% killing efficiency after 1–2 h of illumination depending on the conditions. This suggested that the penetration of the photosensitizer molecules into the cell's interior may be not necessary for triggering of the bacteria inactivating mechanism.

In our study, the *in vitro* photodynamic inactivation of SiO_2–NH_2–RB nanoparticles on gram-positive bacteria has been investigated, using MRSA and *S. epidermidis* as the models for gram-positive bacteria. Gram-positive bacteria were treated with SiO_2–NH_2–RB nanoparticles and various controls, followed by 40 min of light illumination. The controls included bacteria only, bacteria treated with SiO_2–NH_2, and bacteria treated with free RB dye. As shown in figure 5, it appeared that both *S. epidermidis* and *S. aureus* could survive in the presence of amine-functionalized silica nanoparticles (SiO_2–NH_2), when the same

dosage of SiO_2–NH_2 nanoparticles was used as compared with SiO_2–NH_2–RB nanoparticles (~10^5 NPs/bacterium). Free RB showed good killing efficiency (approximately six-orders-of-magnitude reduction in the viable count) on gram-positive bacteria.

We noticed that the free RB solution in our study ([RB] ~3 μM) displayed significantly higher efficiency in killing gram-positive bacteria than reported in the literature [34] ([RB] ~5 μM; less than two-orders-of-magnitude reduction in the viable count; white light illumination of 1.1×10^{-3} einstein m^{-2} s^{-1}). Such improved killing efficiency of RB observed in our experiments was probably due to the higher illumination intensity of our light source (~33 J cm^{-2} in 40 min of 525 nm illumination, equivalent to 1×10^{-4} einstein m^{-2} s^{-1}). We also note that, compared to other reports using SnCe6 as the photosensitizer and a similar illumination intensity (21 J cm^{-2} in 5 min exposure, four–five-orders-of-magnitude reduction in the viability count of MRSA) [36, 37], SiO_2–NH_2–RB nanoparticles again show superior killing efficacy.

More significantly, SiO_2–NH_2–RB were shown to be more potent than free RB in inactivating the gram-positive bacteria, with an additional improvement in killing efficiency: a two-orders-of-magnitude reduction in the viability count. This is an intriguing result, considering that the quantum yield of generating $^1O_2$ of SiO_2–NH_2–RB nanoparticles is lower than that of the free RB and that the amount of RB in SiO_2–NH_2–RB nanoparticles used in this set of experiments is only approximately half of that in the free RB solution. We suggest that this could be due to the higher localization of RB to the cell surface when attached to the SiO_2 nanoparticles, as compared to free RB in solution. The locally concentrated $^1O_2$ generated by the SiO_2–NH_2–RB nanoparticles would likely be more efficient in causing damage to the bacteria even though free RB in solution may generate overall more $^1O_2$. This is consistent with the previous observation that the protoporphyrin IX-loaded silica particles showed a higher efficiency of singlet oxygen generation than the corresponding free porphyrins [38]. The result demonstrates the advantages of nanoparticle-based photosensitizers over the corresponding free photosensitizing molecules in solution.

3.4. Effects of SiO_2–NH_2–RB dosage and illumination time

The effects of the SiO_2–NH_2–RB nanoparticle dosage and the illumination time were investigated. The same number of gram-positive bacteria were either treated with different amounts of SiO_2–NH_2–RB under a constant illumination time or treated with the same amounts of SiO_2–NH_2–RB while varying the illumination time. Control bacterial groups were treated in a similar manner. Ambient light was completely shielded throughout the treatment until the lamp illumination step. The results, shown in figures 6 and 7, indicated that for 10 μl of bacterial suspensions (~10^8 CFU ml^{-1}) under a 525 nm light source of ~14 mW cm^{-2}, approximately 6 mg ml^{-1} of SiO_2–NH_2–RB nanoparticles and 40 min exposure would be required to achieve an eight-orders-of-magnitude reduction in the viability count. This corresponds to a ratio of approximately 10^5 nanoparticles per bacterium.

4. Conclusions

In summary, we report the development of a new type of photosensitizer, RB-decorated silica nanoparticles, which displayed high efficiency in inactivating MRSA and *S.*

epidermidis through photodynamic action. The advantages of these nanoparticle-based photosensitizers over the free photosensitizing molecules include the following: (1) association of the dyes with NPs makes the dyes more resistant toward photobleaching; (2) by concentrating the photosensitizing molecules onto the nanoparticle surface, the locally generated singlet oxygen may reach a higher concentration than when free molecules act individually or in solution; this causes more damage to the target bacteria. The design of attaching photosensitizing molecules to nanoparticles could potentially expand the pool of molecules as photosensitizers in PDT applications. When immobilized onto silica nanoparticles, some molecular dyes that are otherwise insoluble in water, can still be used as photosensitizers in aqueous media. Furthermore, if the nanoparticle surfaces can be modified to become positively charged, or be decorated with target-recognition elements [39], they can become more effective in photodynamically inactivating gram-negative bacteria or more specific toward certain targets. Efforts in this direction are currently underway.

Acknowledgments

This work was partially supported by grant number RR-016480 from the National Center for Research Resources (NCRR) of the National Institutes of Health (NIH).

References

1. Jori G, Brown SB. Photochem Photobiol Sci. 2004; 3:403. [PubMed: 15122355]
2. Jori G, Fabris C, Soncin M, Ferro S, Coppellotti O, Dei D, Fantetti L, Chiti G, Roncucci G. Lasers Surg Med. 2006; 38:468. [PubMed: 16788934]
3. Wainwright M, Crossley KB. Int Biodeterior Biodegr. 2004; 53:119.
4. Qian P, Johan M. Anticancer Res. 2003; 23:3591. [PubMed: 14666654]
5. Asta J, Johan M. Photodiagn Photodyn Ther. 2007; 4:3.
6. Asta J, Johan M. Photodiagn Photodyn Ther. 2007; 4:80.
7. Wesley MS, Cynthia MA, Van Lier JE. Methods Enzymol. 2000; 319:376. [PubMed: 10907528]
8. Malik Z, Hanania J, Nitzan Y. J Photochem Photobiol. 1990; B 5:281.
9. Wainwright M. J Antimicrob Chemother. 1998; 42:13. [PubMed: 9700525]
10. Phillips D. Prog React Kinet. 1997; 22:176.
11. Bertoloni G, Lauro FM, Cortella G, Merchat M. Biochim Biophys Acta. 2000; 1475:169. [PubMed: 10832032]
12. Bhatti M, MacRobert A, Meghji S, Henderson B, Wilson M. Photochem Photobiol. 1998; 68:370. [PubMed: 9747591]
13. Griffiths MA, Wren BW, Wilson M. J Antimicrob Chemother. 1997; 40:873. [PubMed: 9462440]
14. Wilson M, Pratten J. Microbios. 1994; 78:163. [PubMed: 8041293]
15. Wilson M, Yianni C. J Med Microbiol. 1995; 42:62. [PubMed: 7739027]
16. Decraene V, Pratten J, Wilson M. Curr Microbiol. 2008; 57:269. [PubMed: 18587617]
17. Usacheva MN, Teichert MC, Biel MA. Lasers Surg Med. 2001; 29:165. [PubMed: 11553906]
18. Zeina B, Greenman J, Purcell WM, Das B. Br J Dermatol. 2001; 144:274. [PubMed: 11251558]
19. Bhatti M, MacRobert A, Meghji S, Henderson B, Wilson M. Photochem Photobiol. 1997; 65:1026. [PubMed: 9188283]
20. Corbitt TS, Sommer JR, Chemburu S, Ogawa K, Ista LK, Lopez GP, Whitten DG, Schanze KS. ACS Appl Mater Interfaces. 2009; 1:48. [PubMed: 20355752]
21. Hamblin M, Hasan T. Photochem Photobiol Sci. 2004; 3:436. [PubMed: 15122361]
22. Tamagaki S, Liesner CE, Neckers DC. J Org Chem. 1980; 45:1573.
23. Banks JG, Board RG, Carter J, Dodge AD. J Appl Bacteriol. 1985; 58:391. [PubMed: 3997691]

24. Zhang P, Steelant W, Kumar M, Scholfield M. J Am Chem Soc. 2007; 129:4526. [PubMed: 17385866]
25. Larry, LH. Sol–Gel Silica: Properties, Processing and Technology Transfer. Westwood, NJ: Noyes Publications; 1998.
26. Brinker, CJ.; George, WS. Sol–Gel Science: The Physics and Chemistry of Sol–Gel Processing. Boston, MA: Academic; 1990.
27. Jeunieau, L.; Debuigne, F.; Janos, BN. Synthesis of inorganic and organic nanoparticles in microemulsions. In: John, T., editor. Reactions and Synthesis in Surfactant Systems. Vol. 100. New York: Dekker; 2001. p. 609-31.
28. Roger, L.; Mean, JH.; Dinesh, OS. Microemulsions: formation, structure, properties, and novel applications. In: Darsh, TW.; Martin, EG.; Dinesh, OS., editors. Surfactants in Chemical/Process Engineering. Vol. 28. New York: Dekker; 1998. p. 315-67.
29. http://www.rcdc.nd.edu/compilations/qy/QY1169.HTM
30. Tang W, Xu H, Kopelman R, Philbert MA. Photochem Photobiol. 2005; 81:242. [PubMed: 15595888]
31. Yan F, Kopelman R. Photochem Photobiol. 2003; 78:587. [PubMed: 14743867]
32. Irene EK, Robert WR. Methods Enzymol. 2000; 319:9.
33. Schaap AP, Thayer AL, Blossey EC, Neckers DC. J Am Chem Soc. 1975; 97:3741.
34. Dahl TA, Midden WR, Neckers DC. Photochem Photobiol. 1988; 48:607. [PubMed: 3071811]
35. Bezman SA, Burtis PA, Izod TPJ, Thayer MA. Photochem Photobiol. 1978; 28:325. [PubMed: 360250]
36. Embleton ML, Nair SP, Cookson BD, Wilson M. J Antimicrob Chemother. 2002; 50:857. [PubMed: 12461004]
37. Embleton ML, Nair SP, Heywood W, Menon DC, Cookson BD, Wilson M. Antimicrob Agents Chemother. 2005; 49:3690. [PubMed: 16127041]
38. Rossi LM, Silva PR, Vono LLR, Fernandes AU, Tada DB, Baptista MS. Langmuir. 2008; 24:12534. [PubMed: 18834155]
39. Brevet D, et al. Chem Commun. 2009; 12:1475.

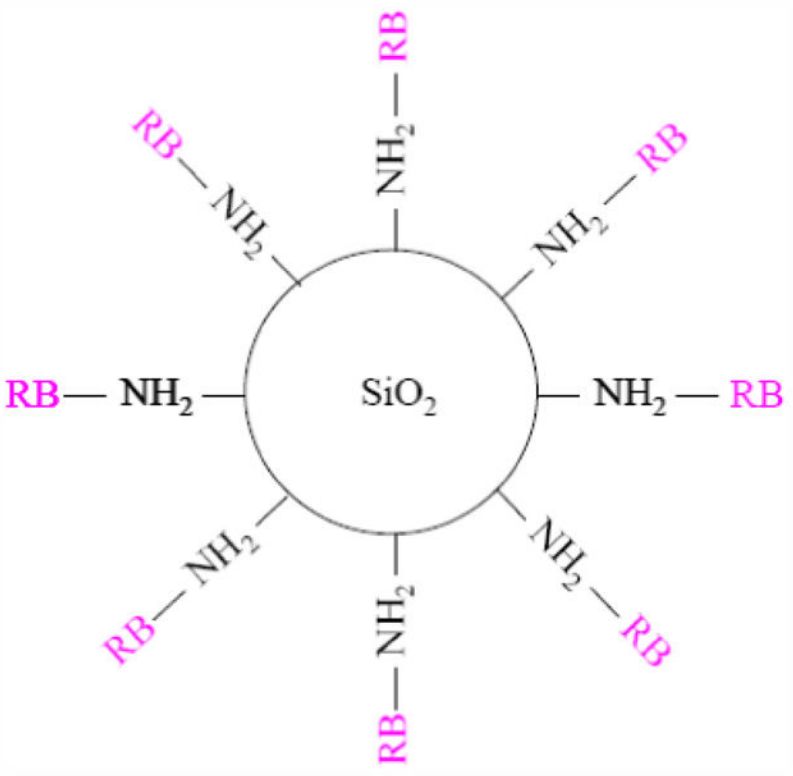

Figure 1.
Schematic of the design of SiO_2–NH_2–RB nanoparticles.

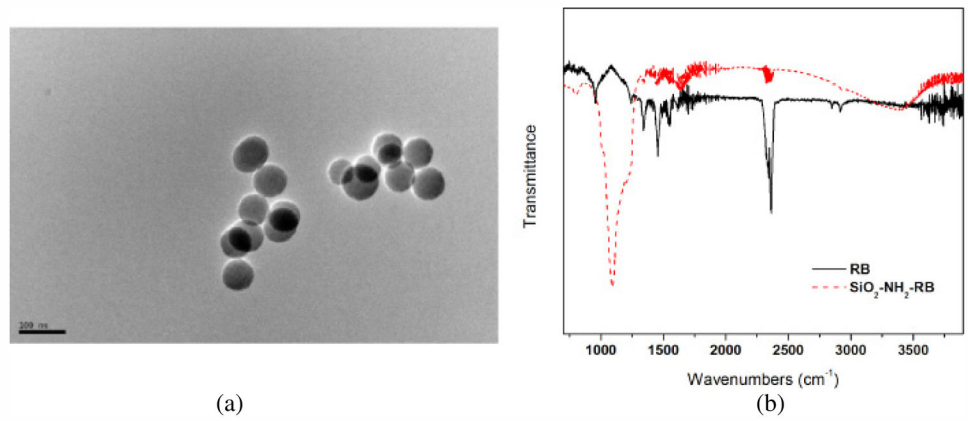

Figure 2.

(a) TEM image of SiO_2–NH_2–RB nanoparticles. (b) IR spectra of SiO_2–NH_2–RB nanoparticles (dot line) and free RB solution (solid line).

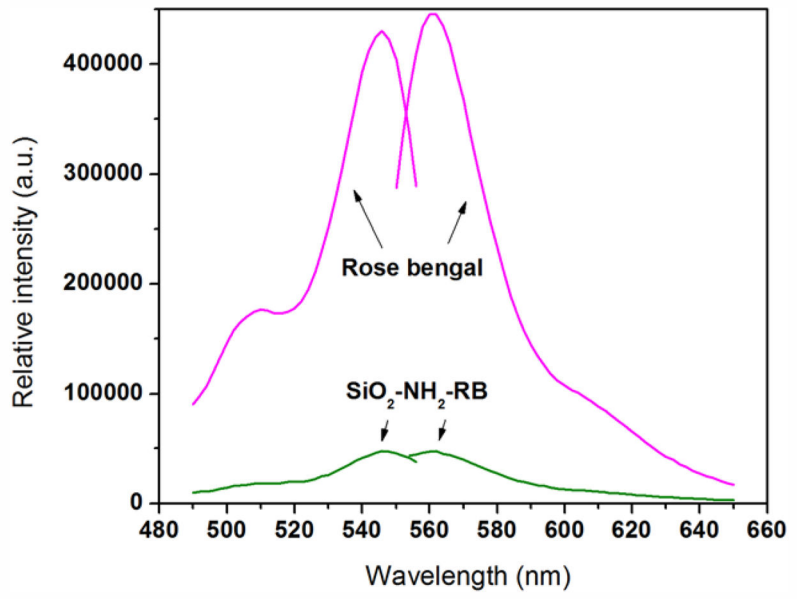

Figure 3.
Excitation and emission spectra of free RB solution and SiO_2–NH_2–RB nanoparticles.

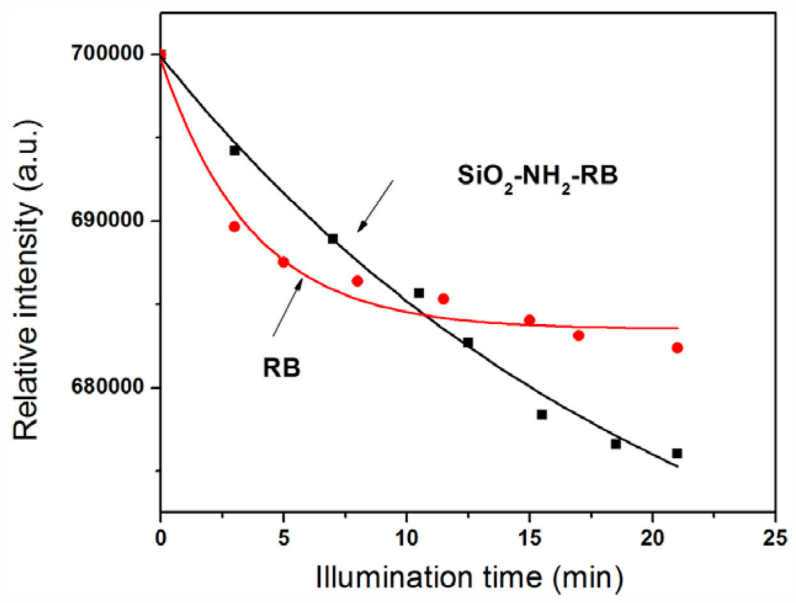

Figure 4.

Change of ADPA fluorescence due to singlet oxygen generated by free RB dye and SiO_2–NH_2–RB nanoparticles under illumination.

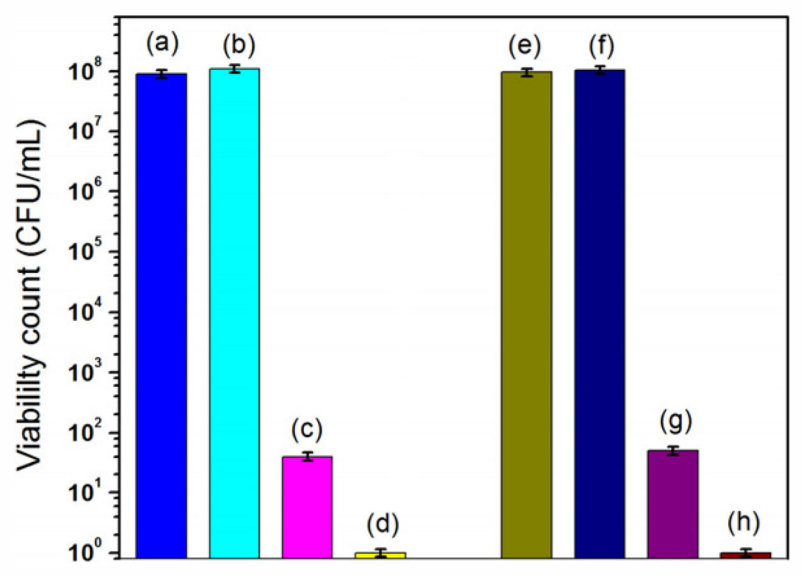

Figure 5.

Viability count of gram-positive bacteria treated with SiO_2–NH_2–RB nanoparticles and controls. (a) *S. epidermidis*; (b) *S. epidermidis* + SiO_2–NH_2; (c) *S. epidermidis* + RB; (d) *S. epidermidis* + SiO_2–NH_2–RB; (e) *S. aureus*; (f) *S. aureus* + SiO_2–NH_2; (g) *S. aureus* + RB; (h) *S. aureus* + SiO_2–NH_2–RB.

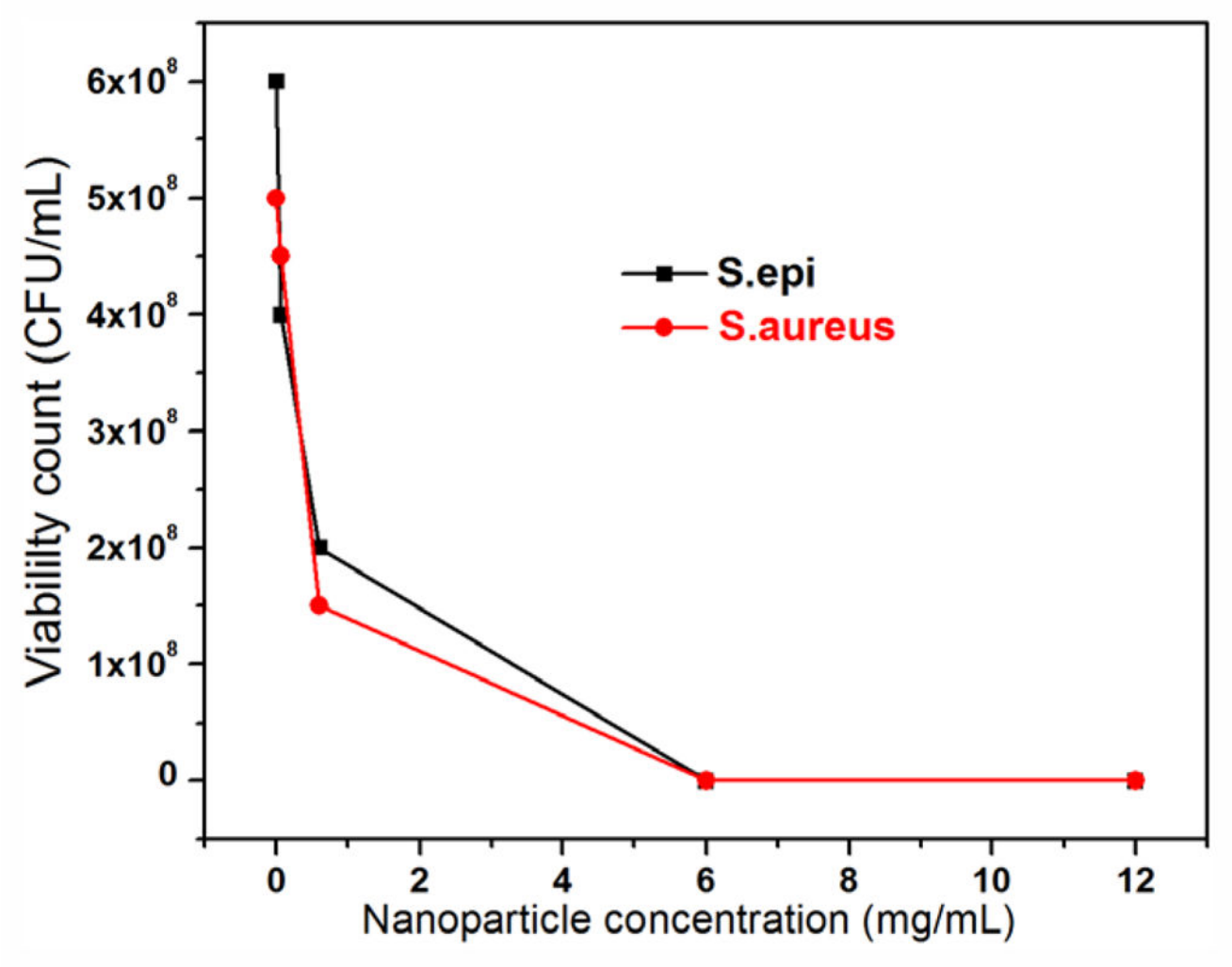

Figure 6.

Viability count of gram-positive bacteria treated with different dosages of SiO_2–NH_2–RB nanoparticles, under a 525 nm light source of 14 mW cm^{-2} for 40 min illumination.

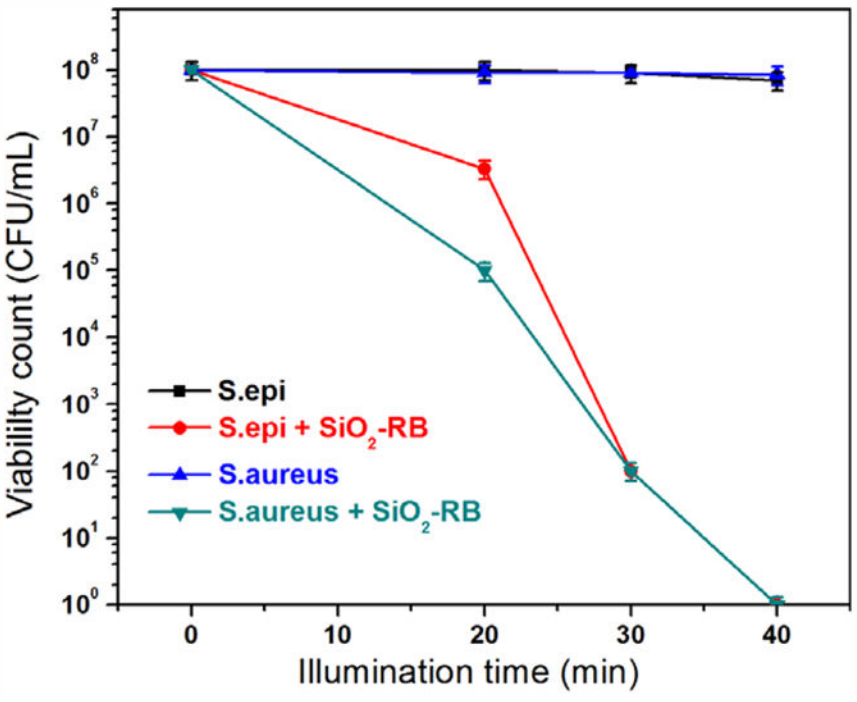

Figure 7.

Viability count of gram-positive bacteria treated with SiO_2–NH_2–RB nanoparticles for different illumination times.